



Biomedical Science
Faculty of Health and Society
Malmö University
SE-205 06 Malmö
Sweden

Master programme in Biomedical Surface Science
<http://edu.mah.se/en/Program/VABSE>

Master degree thesis, 30 ECTS
Examensarbete, 30 hp

THE ROLE OF WATER PURITY IN EMULSIFICATION AND REMOVAL OF OIL FROM SOLID SURFACES

Andriani Tsompou

SUPERVISOR:
Prof. Vitaly Kocherbitov

2021/06/03

ABSTRACT

Detergents are broadly used in our everyday life for cleaning and washing procedures. They are however, a source of water pollution and can have a negative effect on human health and the environment. To reduce their negative impact, a new trend of using only pure water for washing and cleaning applications is being implemented. However, a scientific basis needs to be established first, as the mechanisms and the effectiveness of this method are not fully understood. In this work, we aim to investigate the effect of water purity on the removal of oil from surfaces and the stability of colloidal systems. To do that, two purified water grades are compared with non-purified tap water and 10 mM NaCl solution. Results from *measurement of oil film mass before and after water contact* and *Quartz Crystal Microbalance with Dissipation (QCM-D)* indicate that purified water grades can wash a surface more efficiently than non-purified water grades. *Contact angle measurements* show that pure water facilitates the cleaning process while *spreading of oil* on plastic surfaces indicates that electrostatic interactions have an important role in the system. *Visual observations of o/w emulsions*, show that purified water grades redisperse the oil better. We hypothesize that the mechanism behind the cleaning and washing without detergents relies on the electrostatic interactions. To further investigate the effect of salt on cleaning mechanisms, we performed *zeta potential measurements*. Results indicate that salt has a negative effect on the stability of the particles.

Keywords: ultra-pure water, detergency, detachment of oil from solid surfaces, washing, cleaning

This master thesis has been defended on June 3 2021, at the Faculty of Health and Society, Malmö University.

Opponent: Assoc. Prof. Javier Sotres

Examiner: Prof. Sergey Shleev
Biomedical Science
Faculty of Health and Society
Malmö University

TABLE OF CONTENTS

THE ROLE OF WATER PURITY IN EMULSIFICATION AND REMOVAL OF OIL FROM SOLID SURFACES	1
ABSTRACT	2
TABLE OF CONTENTS	3
INTRODUCTION	4
Roll up mechanism	6
Emulsification - Solubilization	9
Aim	9
MATERIAL AND METHODS	10
MATERIALS	10
Emulsion preparation	10
Visual observations of the state of oil after emulsification	11
Contact angle measurements in a three-phase system	11
Spreading of oil on a plastic surface	11
Dynamic light scattering (DLS)	12
Measurement of oil film mass before and after water contact	12
QCM-D	13
Spin coating	13
QCM-D protocols	13
QCM-D data analysis for film thickness	14
QCM-D data analysis from Protocol A	15
RESULTS	16
QCM-D	16
Measurement of oil film mass before and after water contact	20
Contact angle in a three-phase system (glass surface)	21
Spreading of oil on a plastic surface	22
Visual observations of the state of oil after emulsification	23
Behavior of oil film on a water surface	23
Redispersion	25
Surface and zeta potential of 200 nm and 1 μ m particles	26
DISCUSSION	29
CONCLUSION	33
Acknowledgements	34
REFERENCES	35

INTRODUCTION

Water is an inorganic, tasteless, odorless, transparent, and colorless substance. Two hydrogen atoms and one oxygen atom are connected via covalent bonds in a water molecule [1]. It can be found in a liquid, solid and gaseous state. Without any doubt, it is one of the most important and abundant fluids on Earth. Its importance can be found in many different topics like the climate, the formation of landscapes, biology, and chemistry [2]. Since the old times, Greeks believed that water was the fundamental element of life. In the 6th century BCE, Thales of Miletus wrote *“It is water that, in taking different forms, constitutes the earth, atmosphere, sky, mountains, gods and men, beasts and birds, grass and trees, and animals down to worms, flies and ants. All these are different forms of water. Meditate on water!”*. It was until the 18th century that water was believed to be one of the fundamental elements of life, alongside the earth, air and fire [3].

Its unique properties render water vital for many physical and chemical processes. Its high heat capacity, highest than most of the liquids [4], helps the oceans to store thermal energy making them important for the earth’s temperature. Its high surface tension (the work needed to increase the surface area), 0.072 N/m [4,5], helps the living of many animals and it has also proven important in many industrial processes [6]. Many of its physical properties can be characterized as atypical as they differ from other liquids. An unusual situation is seen when water is found in a solid state. Because of its open structure, many hydrogen bonds can be formed, thus its density decreases [3]. In addition to its properties, water is universally used as a solvent. Many chemical substances can be dissolved in it making it excellent for a variety of uses in many industrial areas [2,7]. One of the areas that water is highly used is cleaning and washing.

Washing is an important aspect of every household nowadays. It is known that the washing procedure works with water and detergent. Detergents are composed of various components, but surfactants and builders are always present as they are both important for the removal of *soils (dirt)* in the cleaning procedure [8]. Surfactants (surface active agents [9]) are compounds that lower the interfacial tension while builders are able to remove ions that may interfere with surfactants and their work [7,8]. The water used for this process is important as the number of ions present in it, can make the washing procedure more complex. Six factors can dictate the quality of the water and these are: 1) water clarity 2) water hardness 3) amount of total dissolved solids 4) iron content 5) pH 6) bicarbonate in water [9].

Water hardness signifies the amount of Ca^{+2} and Mg^{+2} that exists in the water [10]. Their presence in the water affects the cleaning process as they reduce the electrical potential of negatively charged substrates and dirt by binding to them. This, facilitates the redeposition of the soil, surfactants, and soil bound with surfactants [11,12]. Moreover, the reduced electrical potential will promote a screening effect that will allow the soil to approach or even aggregate. Because of these issues, builders are added to the detergents in order to reduce the amount of cations found in the water [13].

Water clarity shows how clear the water is. Most of the water in the rural areas is being cleaned. Total dissolved solids (TDS) is the total amount of mobile charged ions such as minerals, salts and metals dissolved in a specific amount of water and it is measured in parts per millions (ppm). Overall, it shows all the inorganic and organic substances that are present in the water. Iron consistency, pH and bicarbonates can also alter some of the water properties when it comes to washing but in a minor effect [9].

Removing soil from (hard) surfaces is a procedure very important in our everyday life and because of that, it is well studied. There are three main mechanisms that are established for the removal of soil (figure 1). *Detergency* or *surface chemical* processes use surfactants to achieve results. *Mechanical mechanisms* on the contrast are based on physical means such as abrasion while *chemical mechanisms* use solvents for the removal of soil. Although the most used and studied mechanism is detergency, as it offers a more cost-effective approach [7], it usually relies on some degree in mechanical action to achieve the complete removal of soils. A combination of detergency and chemical mechanisms can also be found [14].

Depending on the type of soil which is to be removed the detergency mechanisms can be further categorized (figure 1). Liquid soil can be removed by the ‘*roll up mechanism*’ and the *solubilization* [9]. Depending on the system, one or another mechanism can prevail. The solid inorganic soils can be removed via *wetting* mechanism while the organic solid soil such as waxes, fat and grease can be *liquified* by applying heat [9].

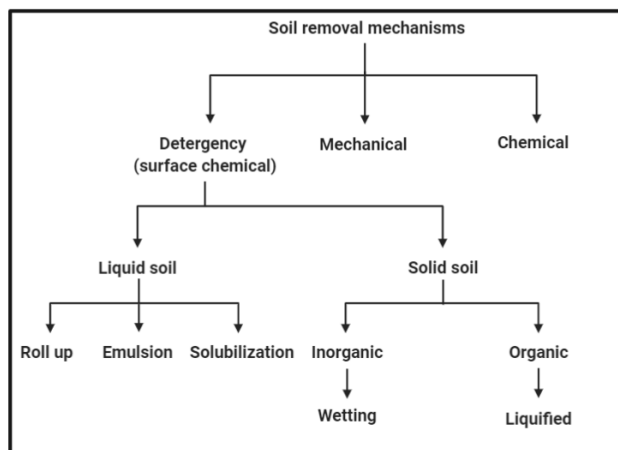


Figure 1: Major mechanisms involved in removal of soils from surfaces [14]

During the cleaning procedure, the liquid soils are dispersed in a liquid medium and they create emulsions. Emulsions tend to be thermodynamically unstable and in unknown time they can phase separate into two continuous phases due to several processes. These include, coagulation where the soil is aggregated, creaming or sedimentation (which can occur for the soil that is not aggregated) and coalescence where the soil merges [15].

Many forces, such as electrostatic interactions, van der Waals, hydration and steric forces are important for the stability of an emulsion. DLVO theory (Derjaguin-

Landau-Verwey-Overbeek theory) assumes a balance between the repulsive and the attractive forces that are formed on the electrical double layer (EDL) of each dirt particle. Repulsive electrostatic interactions are due either to same charged double layer that surrounds the particles or to particle-solvent interactions. Van der Waals forces are believed to be the attractive forces [9,16]. For the particles to be dispersed, the repulsive interactions must prevail the attractive ones while for aggregation, the opposite must occur [17]. An important factor for the emulsion stability is the surface potential which is hard to be experimentally found. Instead, the zeta potential (figure 2) is broadly used for characterizing particle stability. Particles can interact with the liquid in the slipping plane which is the boundary between the hydrodynamic mobile (bulk) and immobile fluid (particle and Stern layer) and is where zeta potential is found. Particles are considered stable when zeta potential is above + 30 mV or below -30 mV. Small changes in pH or in salt concentration can have a dramatic effect on zeta potential [18–20].

Emulsions can achieve stability either by inducing charge on the surfaces or by using surfactants. The use of surfactants (emulsifiers) is common when emulsion stability needs to be achieved.

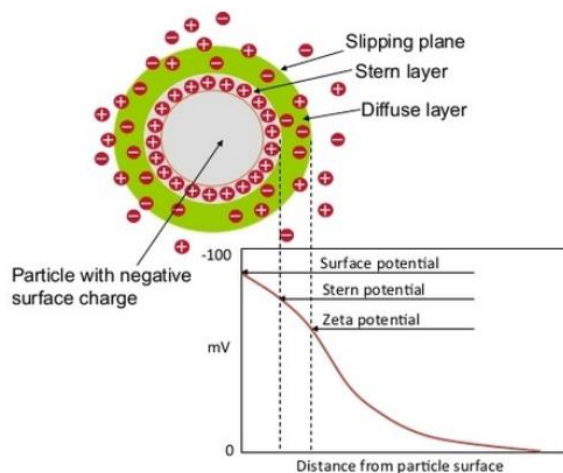


Figure 2: Electrical double layer formation in a negative surface charged particle. Stern layer is formed by specific adsorption of ions and molecules and it is an immobile layer. Diffuse layer is formed by non-specific adsorbed ions. Slipping plane is the boundary between the immobile and the mobile fluid [21].

Based on the emulsion stability rules, the soil removal mechanisms take advantage of the stability that surfactants promote and clean the surfaces. The mechanisms that we will focus on are: i) roll up mechanism [8,9,22,23] ii) emulsification-solubilization [8,9,23]. Through these mechanisms, surfactants can 1) facilitate the removal of dirt from the surface 2) solubilize or disperse dirt, and help to prevent its redeposition [16].

Roll up mechanism

The removal of soil (oil) is achieved by submerging the surface in an aqueous bath. The wetting of the soil can eventually lift it and clean the surface. The contact angle that the soil creates with the surface is a key component of the roll up mechanism. In the bath, the contact angle that the soil makes with the substrate is increased by

adsorption of the surfactant. The work, W , needed to keep the dirt, D , away from the surface, S , is called work of adhesion and is defined as the work required to increase the bath dirt (BD), and bath surface (BS) interfaces by reducing the dirt surface (DS) interface (figure 3) [8,22].

$$W_{ad} = \gamma_{BD} + \gamma_{BS} - \gamma_{DS} \quad (1)$$

Where γ is the interfacial tension. Eq. 1 can be also written as:

$$W_{ad} = \gamma_{BD} (\cos\theta + 1) \quad (2)$$

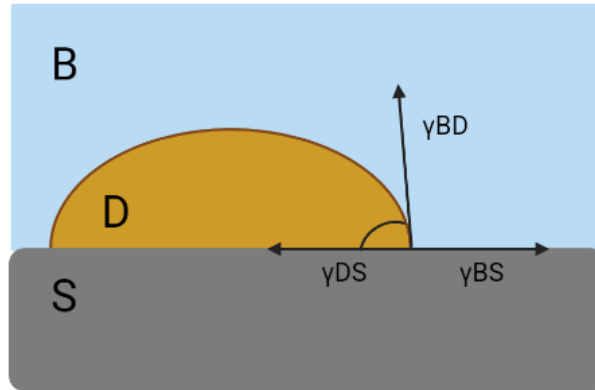


Figure 3: explanation of Young-Dupre equation. Surface (S), Bath (B), Dirt(D)

Equation 2 is the Young- Dupre equation that allows to calculate the work needed to separate the dirt from the substrate in terms of the contact angle θ . The contact angle can also be found by equation (3):

$$\cos\theta = \frac{(\gamma_{BS} - \gamma_{DS})}{\gamma_{BD}} \quad (3)$$

The addition of surfactant into the bath-surface-dirt system can alter the contact angle, contributing to three different scenarios (figure 4): 1) if the contact angle is 180° the liquid dirt will be completely dispersed in the bath spontaneously 2) if the contact angle is between 90° and 180° then the W_{ad} will be decreased in comparison to the W_{ad} before adding the surfactant but the dirt will not be dispersed in the bath. Mechanical energy is needed to achieve that [24–26] 3) if the contact angle is less than 90° , part of the dirt will remain attached to the surface [8,9,26].

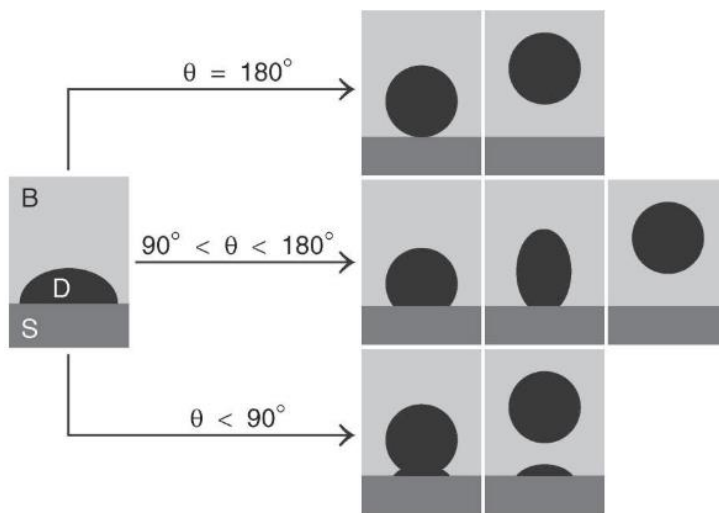


Figure 4: The sequences above illustrate how the liquid dirt (D) attached to the surface (S) rearranges itself after the addition of the surfactant to the bath (B) [8]

The properties of both the surface and the surfactant used are important. For hydrophilic surfaces like glass and cotton the contact angle is more than 90° ($\cos\theta < 0$). When anionic surfactants are used, they orient their charged head group towards the bath leaving the hydrophobic tail in contact with the dirt. Since the contact angle lies between 90° and 180° the roll up mechanism will take place and the dirt will be displaced. In case of a hydrophobic surface, as polystyrene, the contact angle will be less than 90° meaning that a small portion of the dirt will remain attached to the surface. It has been observed by many scientists that the surfactant in these cases cannot reach the surface as it is completely covered with the liquid dirt [23].

Nonionic surfactants have been proven to be more effective than ionic in the removal of oily soil from relatively nonpolar substrates (polyester, nylon). On cotton, however, a relatively hydrophilic fiber, anionics can outperform nonionics in detergency, and both are superior to cationics [27]. The effects here may be due to differences in the orientation of adsorption of the different types of surfactants on the different substrates [9].

Apart from the hydrophilicity/phobicity of the surface, the charge is also an important factor to consider. When the surface is in contact with an aqueous bath it is often negatively charged as the cations are normally more hydrated than the ions. This hydration leads the cations to resign in the bulk whereas the smallest, less hydrated ions tend to specifically adsorb on the surface. Anionic surfactants would orient themselves in a way that the tail is in contact with the substrate or the dirt while the head would be found in the medium. This orientation is governed by the van der Waals interactions between the hydrocarbon chain and the substrate or dirt of a generally hydrophobic nature. If the surfactant is nonionic the orientation would be the same only this time it will be driven by the steric interactions between the head groups. If the surfactant is cationic then the orientation would be the opposite as the head would be in contact with the negatively charged substrate and the dirt, due to electrostatic forces. This orientation promotes the re attachment of dirt on the surface [28].

Emulsification - Solubilization

Emulsions are important for preventing the redispersion of soil on the surface. For the emulsions to be stable, emulsifiers (surfactants) must be used. As the surfactants orient themselves in the emulsion, they create steric or electric barriers that prevent the coalescence and the redeposition of soil (figure 5) [8]. Its purpose is to keep the dirt in the emulsion.

Moreover, detergents act as emulsifiers which can stabilize an emulsion by lowering the dirt-bath interfacial tension. Interfacial tension is the force required to reversibly enlarge the interfacial area [15]. This leads to a reduction in free energy and hence the stabilization of the emulsion by making the emulsification of the oily soils possible [15,23].

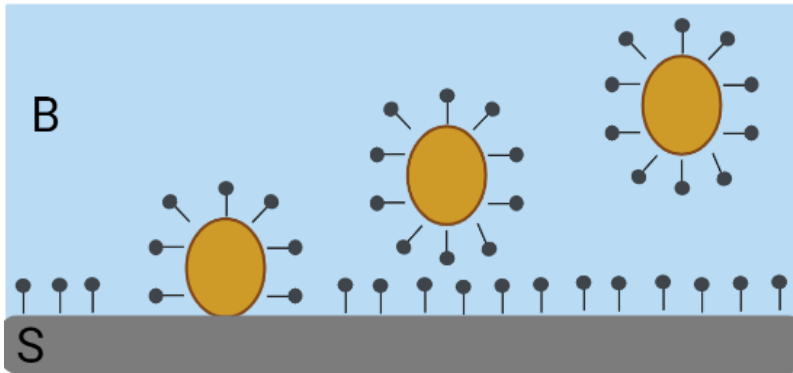


Figure 5: Orientation of surfactant favor the separation of dirt and the substrate. The formulation of micelles helps the solubilization the dirt. Surface (S), Bath (B).

To prevent redeposition of dirt, surfactant molecules adsorb on to the dirt particles in the solution. Their hydrophobic tail dissolves in the dirt and the head group is in contact with water (figure 5). Charged head groups in the anionic surfactant component of detergent formulations lead to electrostatic repulsions between solubilized dirt particles, preventing precipitation. For nonionic surfactants, the head group leads to a hydration barrier, a depletion of water close to the head group, which reduces contact between surfactant-solubilized dirt particles. The surfactant left adsorbed on the surface will also prevent redeposition due to electrostatic or steric repulsions [16].

Aim

Although detergents are broadly used, they can damage the human health and the environment [7]. A way of reducing the detergent usage is by washing only with pure water. But how can the mechanisms of detergency be altered when instead of tap water with detergent, an ultrapure water is solely used?

In this master thesis, we aim to examine the effect of water purity on the stability of colloidal systems and the removal of oil from surfaces. We will focus on finding the differences from a physicochemical point of view between *purified water grades* and *non-purified water grades*. As purified grades, MQ and DIRO are used. MQ is mainly used in the laboratories and DIRO is an ultra-pure water commercially available. *Non-purified* water grades are tap water, which is mainly used in

households, and 10 mM NaCl solution. The final goal is to get additional knowledge about the cleaning procedure mechanisms when only water is used. Proving that detergent-free cleaning is possible, can be of great importance in the biomedical field as it can decrease drastically allergic reactions and skin irritation caused by various laundry detergents [29–31]. Moreover, during the current pandemic situation because of SARS-CoV-2, it is important to possess a better understanding of the basics of washing and cleaning mechanisms for prevention of disease spreading.

MATERIAL AND METHODS

Materials

Four different water grades were used. These are:

- MQ: pure water; mainly used for laboratory purposes. It is produced using PURELAB flex (ELGA, UK)
- DIRO: ultra-pure water provided by SWATAB company (Malmö)
- TAP: tap water from Forskaren building, Malmö
- NaCl: 10 mM NaCl solution in MQ water. Concentration will be provided if different than 10 mM

Two different oil types were used:

- Olive oil: Extra virgin olive oil from Spain (FONTANA est 1978, classic)
- Hexadecane: hexadecane anhydrous, 99+% (Sigma-Aldrich, Germany)

If only one of two oils is used in some experiment, it will be specified. If both oil types are used, they will be referred to as *oil*.

Hydrophobic Oil red O dye LOT: 69H3520, CI: 26125, Solvent Red 27, sodium dodecyl sulfate, sodium chloride and toluene were purchased from Sigma-Aldrich, Germany. Polystyrene nano-/microspheres, sizes: 200 nm and 1 μm from Alpha Nanotech Inc, Canada. Vaseline purchased from Carl ROTH (Germany) and petri dishes PS from VWR (Sweden).

DIRO water was stored in plastic 20 L bottles while NaCl solutions were stored in glass bottles. For each experiment, a small amount of each water grade was poured in a new 50 mL or 15 mL tube which was first rinsed with the same water grade. All tubes that were used more than once were washed with the water grade that they were filled, to minimize contamination. Each new tube was first rinsed with the respective water.

Emulsion preparation

For visual observations, the oils were stained with the hydrophobic dye, Oil red O. In 29 g of oil 0.025 g of dye were dissolved. Both plastic and glass tubes were used. Four emulsions were made at each time. All had the same concentration, the same tube material but different water grade. In that way, the emulsions were observed with the same time difference. Before the preparation, each tube was rinsed with the respective water grade. In a typical experiment, 4 emulsions of 0.3 wt% oil in different water grades were prepared (MQ, DIRO, TAP, NaCl) in plastic/glass tubes.

Emulsions were shaken simultaneously by hand for 10 seconds. Before shaking, the glass tubes were sealed with parafilm.

Visual observations of the state of oil after emulsification

Creaming observations started right after the emulsion preparation. Once the emulsions were ready the tubes were placed on the bench and photos were obtained on average 2 and 30 minutes after the emulsion preparation. After 30 minutes, the tubes were gently shaken to detect redispersion of oil into the aqueous phase.

All observation results were obtained via Xiaomi Redmi Note 8 smartphone. Photos were taken for the visual observation analysis and videos for the redispersion analysis. The photos found on the results are the ones explaining the observations the best.

Contact angle measurements in a three-phase system

The Drop Shape Analysis System-DSA100 (Kruss, Germany) was used for the measurement of contact angle. A 5 μl oil droplet was placed at the middle of a glass surface. The glass was previously cleaned with ethanol, deionized water and dried with N_2 gas. 3 ml of a water grade were added, and the contact angle was measured.

For the measurement of the contact angle, two analytical methods were used: *Circle analysis*: the method is measuring the contact angle by fitting the droplet to a circular segment function. *Drop analysis*: Young-Laplace equation fitting. The model includes a correction which considers both the interfacial effect and the weight of the liquid as reasons for the formation of the droplet. Contact angle is determined by the slope at the three-phase contact point. Theoretically most exact method for calculation of droplet size. Both methods are available in the Drop Shape Analysis System-DSA100 and ImageJ. In Image J they can be found as plugins: drop analysis [32], circle analysis [33]. More than three samples were measured for each occasion. Mean value and standard deviation were calculated in Excel.

Spreading of oil on a plastic surface

A 11x11 cm polystyrene surface, cut from a petri dish, was cleaned with ethanol, deionized water and dried with N_2 gas. A 5 μl oil droplet was placed at the middle of the plastic and 3 ml of a water grade were added. Photos were taken inside the fume hood.

All results were obtained via Xiaomi Redmi Note 8 smartphone. All photos were taken from the exact same position in the fume hood. Area (cm^2) analysis was done by ImageJ function of 'area'. The thickness of the droplet was calculated using equation (4):

$$\text{Thickness} = \frac{\text{Volume (cm}^3\text{)}}{\text{Area (cm}^2\text{)}} \quad (4)$$

where the volume of each oil droplet is $5 \mu\text{l} = 5 * 10^{-3} \text{ cm}^3$. Mean value and standard deviation were calculated in Excel.

Dynamic Light Scattering (DLS)

DLS calculates the hydrodynamic size and zeta potential (mV) of particles. The method is based on the random movement of the particles which results from its collisions with solvent molecules. This movement is called Brownian motion and it causes the laser light to scatter at different intensities. By analyzing these intensities the velocity of the particles and hence the particle size can be found through Stokes-Einstein equation [34]. Zeta potential is found indirectly through the electrophoretic mobility (velocity of a particle when subjected to an electrical field) [20].

Size and zeta potential of the nanoparticles were determined by using Zetasizer Ultra (Malvern Instruments, UK). Two polystyrene particle sizes were used, 200 nm and 1 μm . For the 200 nm particles the concentrations used were: 0.05, 0.075, 0.1, 0.2, 1 mg/ml. For 1 μm particles the concentrations used were: 0.01, 0.02, 0.05, 0.1 mg/ml. By using these concentrations, the multiple scattering effects from dense solutions were avoided. For size measurement the DTS0012 cuvette was used. For zeta potential the DTS1080 cuvette was used. The refractive index and absorption values used for calculations are 1.59 and 0.01, respectively. All measurements were done at room temperature (25°C) and three or more measurements were taken from each sample.

For the zeta potential measurements in a series of NaCl concentrations two protocols were used:

Protocol 1:

All water grades were i) filtrated (0.2 μm PETE) ii) not filtrated. 0.05 mg/ml of 1 μm particles and 0.1 mg/ml of 200 nm particles were prepared in a series of 0-20 mM NaCl concentrations. Purified water grades, such as MQ and DIRO, where the presence of ions is limited, were considered as the 0 mM NaCl samples.

Protocol 2:

Water grades were not filtrated. All mentioned particle concentrations (0.05, 0.075, 0.1, 0.2, 1 mg/ml for 200 nm and 0.01, 0.02, 0.05, 0.1 mg/ml for 1 μm particles) were prepared in 0-2 mM NaCl concentrations. Both MQ and DIRO water were used as 0 mM concentration.

Nanoparticles were diluted in each concentration and added into a 2 ml Eppendorf. The Eppendorfs were shaken for 10 seconds. The sample preparation took place right before the measurement so as the time between the measurements to be the same for all samples. For each measurement 1 mL of sample was inserted into the cuvette. After each measurement, the cuvette was cleaned with ethanol and deionized water.

Measurement of oil film mass before and after water contact

To detect the washing efficiency of each water grade in different tube materials, the oil film before and after contact with water was measured. The procedure was performed on 15 mL plastic and glass tubes. In each step the mass of the tube was measured and written down. In the plastic tube the lid was also measured with the tube. The Mettler Toledo AT261 analytical balance (Marshall Scientific, USA) was used for all measurements.

First, an empty tube was measured (g). A substantial amount of *olive oil* was placed on the surface of the tube and with the help of a cotton stick it was spread on the whole surface. The final olive oil amount in the tube should be between 14-15 mg. 5 g of water were added. The tube was vortexed for i)10 or ii) 20 seconds and the water was gently discarded. Before vortex, the glass tubes were covered with parafilm. The tube was remeasured and kept one day in the fume hood with the lid open and one day on the desiccator (molecular sieves, 3 Å) to completely dry. Glass tubes stayed on the desiccator 2 days until completely dry. The final mass of the tube was measured, and the loss of oil was calculated by subtracting the g of the tube after drying from the g after the addition of oil.

Results from 10 and 20 seconds in the vortex did not show significant difference thus only the experiment with 20 seconds in the vortex will be shown.

QCM-D

All measurements were performed using the Q-Sense QCM-D E4 unit equipped with a standard flow module (Biolin Scientific AB, Sweden). The instrument is based on the QCM-D technology which enables a real-time monitoring of mass, thickness, and viscoelastic properties of the film deposited on the sensor. All measurements were performed and measured at 25 °C and the pump speed was 0.25 ml/min. The QSX 303 SiO₂ QCM-D sensors were washed with water and ethanol before used. Reused sensors were rinsed with MQ water, 2% SDS in MQ water, ethanol, acetone and MQ. Next, they were dried with N₂ gas and finally treated with UV radiation for 10 minutes. If the sensors were not clean after this procedure, they were immersed in toluene for 30-40 minutes, rinsed with MQ, dried with N₂ gas, and then treated with UV radiation for 10 minutes.

Spin coating

Spin coating was used to deposit the vaseline sample on the quartz sensor. 10 µl of vaseline in toluene were deposited onto the QSX 303 SiO₂ QCM-D sensor (5 MHz) (Biolin Scientific AB, Sweden) by dissolving 0.02 ml of the initial sample in 0.08 ml toluene solvent. The initial sample was 0.2 g of vaseline in 3 g of toluene. The organic solvent was left to evaporate in the fume hood for 15 minutes and another 30 minutes in the desiccator.

QCM-D protocols

Protocol in liquid (L): measurements were performed in liquid medium

- 1) Measure an empty sensor in air for 10 minutes
- 2) Measure an empty sensor in water (MQ-DIRO-TAP-10 Mm NaCl) for 10 minutes each
- 3) Spin-coat the same sensor
- 4) Measure the coated sensor in air for 10 minutes
- 5) Measure the coated sensor in a water medium for 40 minutes
- 6) Measure the coated sensor in 4 g/L SDS medium for 10-20 minutes

- 7) Measure the coated sensor in MQ water for 10-20 minutes
- 8) Measure the coated sensor in air for 10 minutes

To achieve more robust results, protocol in Air (A) was introduced. Protocol A was introduced as to determine the statistical differences and if the water grades can clean the coated sensor.

Protocol in air(A): measurements were performed in air medium

- 1) An empty sensor was measured in air for 10 minutes (**x5**). Between each measurement the sensor was removed and mounted again
- 2) The same sensor was spin-coated and measured in air for 10 minutes (**x5**). Between each measurement the sensor was removed and mounted again
- 3) The properties of the film in air were examined
 - A. If the overtones deviated less than 10% the experiment would continue
 - B. If the overtones deviated more than 10% then the sensor was cleaned. Return to step 1.
- 4) Start experiment with one water grade for 40 minutes (MQ, DIRO, TAP, 10 mM NaCl, 4 g/L SDS in MQ water)
- 5) The sensor was dismantled and washed gently with water to remove NaCl (if used)
- 6) The sensor was dried with N₂ gas and left for 10 minutes in the desiccator to completely dry
- 7) The film was measured again in air for 10 minutes (**x5**)

The measurements were performed 5 times in order to eliminate the error that occurs from the assembly of the apparatus.

QCM-D data analysis for film thickness

The heart of the QCM-D technology is a quartz disc. Quartz is a piezoelectric material that can be made to oscillate at a defined frequency by applying an appropriate voltage via metal electrodes. The frequency of oscillation can be affected by the addition or removal of small amounts of mass onto the electrode surface. Under the assumption that the material was homogeneously distributed over the sensor area, the mass of the dry film was determined by using the Sauerbrey equation (5) and the thickness was calculated by equation (6).

$$\Delta f_n = \frac{2f_0^2 m}{Z_q} \quad (5)$$

$$t = \frac{V}{A} = \frac{m}{A\rho} \quad (6)$$

Where Δf_n is the frequency change normalized per overtone n. The overtone number ranges between the odd numbers from 1-13. m is the areal mass (kg m⁻²), Z_q is the acoustic impedance of quartz ($Z_q = 8.8 \cdot 10^6$ kg m⁻² s⁻¹), f_0 is the fundamental resonance frequency of the quartz sensor (≈ 5 MHz), t is the thickness of the dry film, V is the

volume, A is the area, m/A is the Sauerbrey mass and ρ is the density. A density of 900 kg/m^3 was used for vaseline.

QCM-D data analysis for Protocol A

The obtained raw data was analyzed using MATLAB. To determine the thickness of the film before and after washing it with water, the mean value of the five measurements for each regime was calculated. First, equation (7) was used to calculate the mean frequency of each overtone for each sample for all 5 measurements:

$$\bar{f}_n s = \frac{1}{5} \sum_{i=1}^5 f_n(s, i) \quad (7)$$

Where $\bar{f}_n s$ is the mean frequency of each overtone, normalized per overtone, for each sample s ($s=e$ -empty sensor, c -coated film, t -treated with water film) of all measurements i . $f_n(s, i)$ is the mean frequency of each overtone n , for each sample and each measurement i . To detect the frequency of the coated sensor before and after water treatment eq. (8) and eq (9) were used. The frequency of the washed film is calculated by equation (10).

$$\Delta \bar{f}_n c = \bar{f}_n c - \bar{f}_n e \quad (8)$$

$$\Delta \bar{f}_n t = \bar{f}_n t - \bar{f}_n e \quad (9)$$

$$\Delta \bar{f}_n w = \bar{f}_n c - \bar{f}_n t \quad (10)$$

Where $\Delta \bar{f}_n c$ is the frequency of the *coated sensor* for each overtone with respect to the uncoated sensor, $\bar{f}_n c$ is the mean frequency of the coated film. $\Delta \bar{f}_n t$ is the frequency of the *treated coated sensor* for each overtone with respect to the uncoated sensor and $\bar{f}_n t$ is the mean frequency of the film when it is treated with water. $\bar{f}_n e$ is the mean frequency of the empty sensor. $\Delta \bar{f}_n w$ is the frequency for the *washed film* for each overtone.

The standard deviation for $\Delta \bar{f}_n c$, $\Delta \bar{f}_n t$ and $\Delta \bar{f}_n w$ was calculated:

$$\text{std}(\Delta \bar{f}_n c) = \sqrt{[\text{std}(\bar{f}_n c)]^2 + [\text{std}(\bar{f}_n e)]^2} \quad (11)$$

$$\text{std}(\Delta \bar{f}_n t) = \sqrt{[\text{std}(\bar{f}_n t)]^2 + \text{std}[(\bar{f}_n e)]^2} \quad (12)$$

$$\text{std}(\Delta \bar{f}_n w) = \sqrt{[\text{std}(\bar{f}_n c)]^2 + [\text{std}(\bar{f}_n t)]^2} \quad (13)$$

To ensure that the overtone frequencies did not exhibit an odd behavior throughout the experiment, the percentage of the washed vaseline in regard to each overtone is found from equation (14). Consistency of the values is shown in figure 6.

$$\text{washed vaseline (\%)} = \Delta \bar{f}_n w (\%) = (\Delta \bar{f}_n w * 100) / \Delta \bar{f}_n c \quad (14)$$

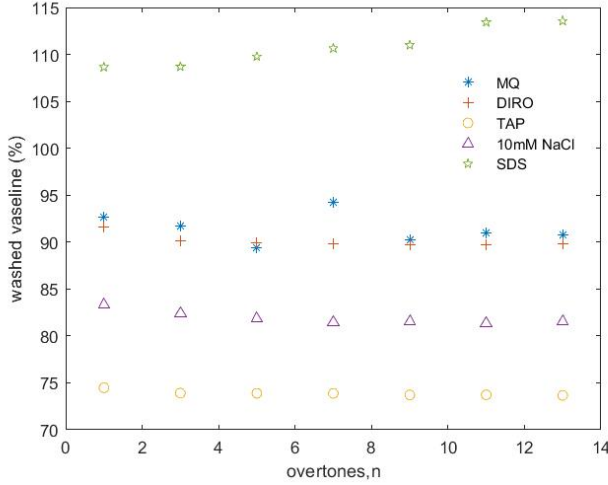


Figure 6: Percentage of washed vaseline for each water grade for each overtone

The fraction of the removed vaseline, $\Delta \bar{f}_n w$, was calculated by equation 15:

$$\Delta \bar{f}_n w = \frac{1}{7} \sum_{n=1}^{13} \Delta \bar{f}_n w (\%) \quad (15)$$

Where $n= 1,3,5,7,9,11,13$. The thickness of each film was calculated by averaging the $\Delta \bar{f}_n s$ of all overtones:

$$\Delta \bar{f}_n s = \frac{1}{7} \sum_{n=1}^{13} \Delta \bar{f}_n s \quad (16)$$

$\Delta \bar{f}_n c$ and $\Delta \bar{f}_n t$ were implemented in equations (5,6) and the thickness was found.

RESULTS

QCM-D

QCM-D method was used to investigate the washing efficiency of the water grades. Results from *Protocol L* for washing a vaseline coated sensor with water, follow the pattern of figure 7. The experiments were done both with all water grades in a row and for each water grade separately. Figure 7 shows the experiment of the washing procedure with MQ water. The film thickness in this type of experiments was measured using the equations 5 and 6 in the frequency of the 3rd overtone. It is shown

that there is no substantial change in the frequencies when the experiment is done in a water medium. All 16 experiments of this type follow the same pattern. An advantage of this method is that it is now known that the washing of the sensor cannot be observed in a water medium regime.

To further investigate the washing procedure, Protocol A was introduced. In this protocol, the measurements were done in air. The results for each water grade are shown below (figures 8-12). By using this protocol, differences in the film thickness are seen in all experiments. Figure 13 shows the percentage of the washed vaseline for each experiment.

Non-purified water grades wash away less than 80% of the vaseline while purified water grades show more than 90% efficiency (figure 13). 4 g/L of SDS in MQ water was used as a comparison. SDS results indicate that the frequency after the washing circle has a negative value (more than 100% washing efficiency).

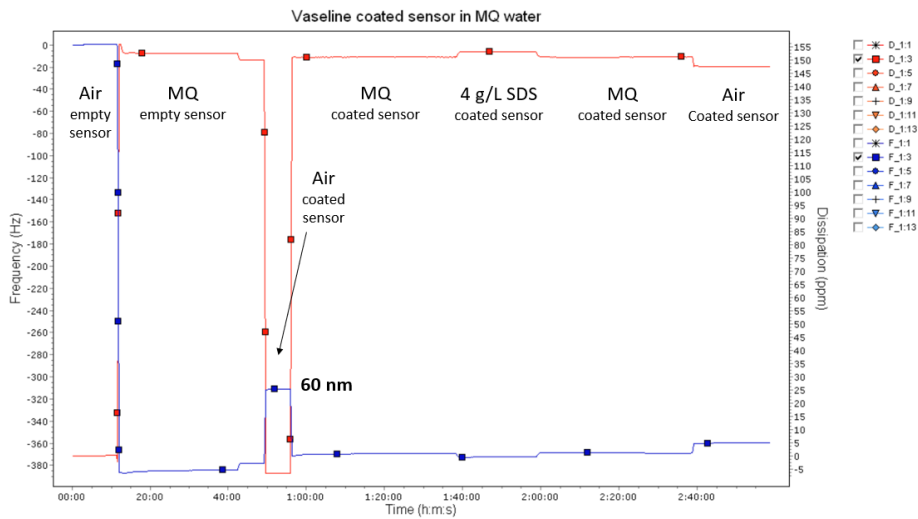


Figure 7: QCM-D experiment in MQ water. The film thickness (60nm) was measured using eq. 5 and 6 for the 3rd overtone. Frequency (blue) and dissipation (red) from the 3rd overtone is shown in the graph.

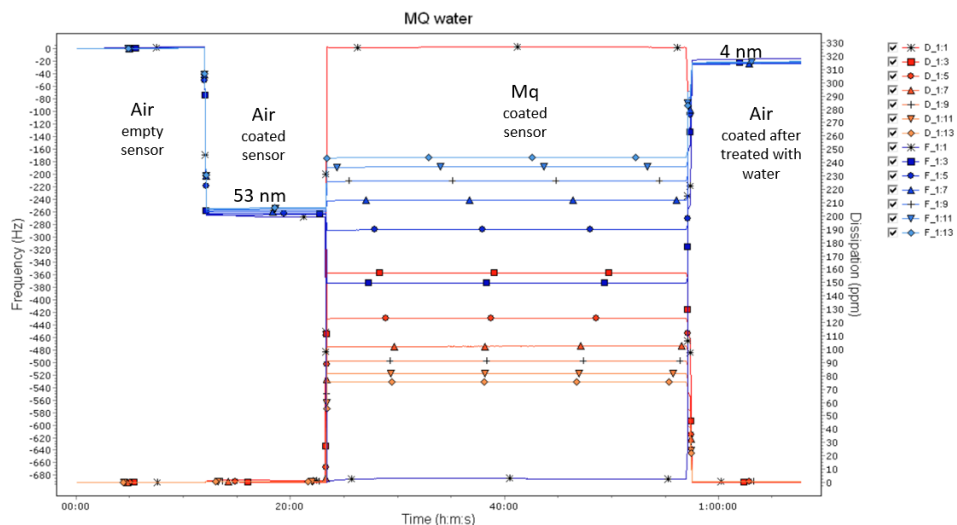


Figure 8: Protocol A for MQ water. Frequency (blue) and dissipation (red) of all overtones is shown. The four regimes are: 1 - empty sensor in air, 2 -sensor with vaseline film (coated) in air, 3 - sensor with vaseline film in MQ water, 4 – dried sensor after treatment with water. One measurement of each regime is shown. n=1

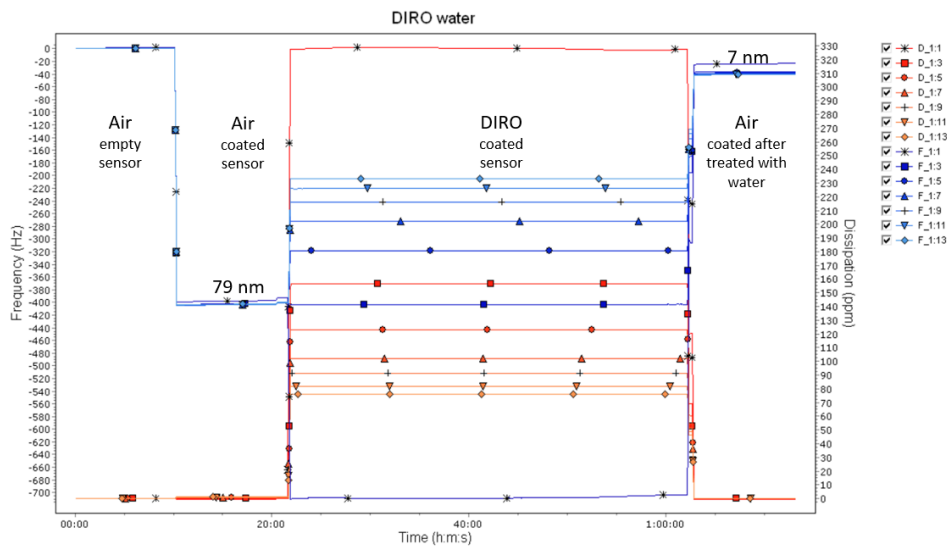


Figure 9: Protocol A for DIRO water. Frequency (blue) and dissipation (red) of all overtones is shown. The four regimes are: 1 - empty sensor in air, 2 -sensor with vaseline film (coated) in air, 3 - sensor with vaseline film in DIRO water, 4 – dried sensor after treatment with water. One measurement of each regime is shown. n=1

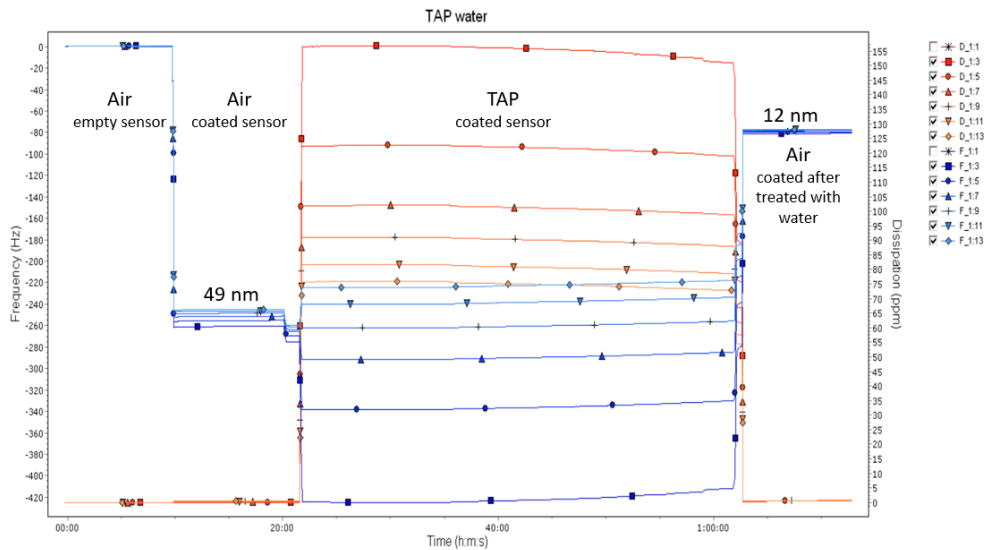


Figure 10: Protocol A for TAP water. Frequency (blue) and dissipation (red) of overtones 3-13 is shown. The four regimes are: 1 - empty sensor in air, 2 -sensor with vaseline film (coated) in air, 3 - sensor with vaseline film in TAP water, 4 – dried sensor after treatment with water. One measurement of each regime is shown. n=1

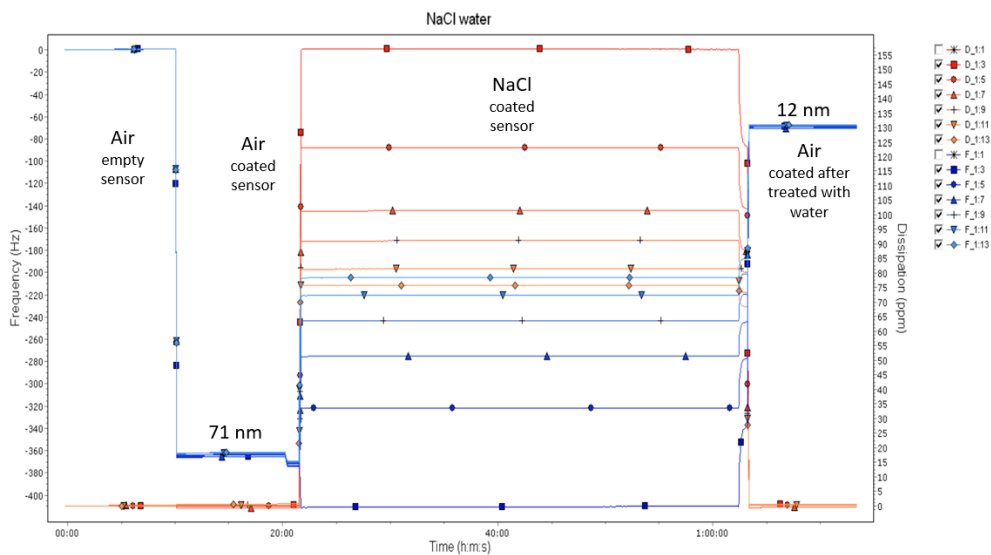


Figure 11: Protocol A for NaCl water. Frequency (blue) and dissipation (red) of overtones 3-13 is shown. The four regimes are: 1 - empty sensor in air, 2 -sensor with vaseline film (coated) in air, 3 - sensor with vaseline film in NaCl water, 4 – dried sensor after treatment with water. One measurement of each regime is shown. n=1

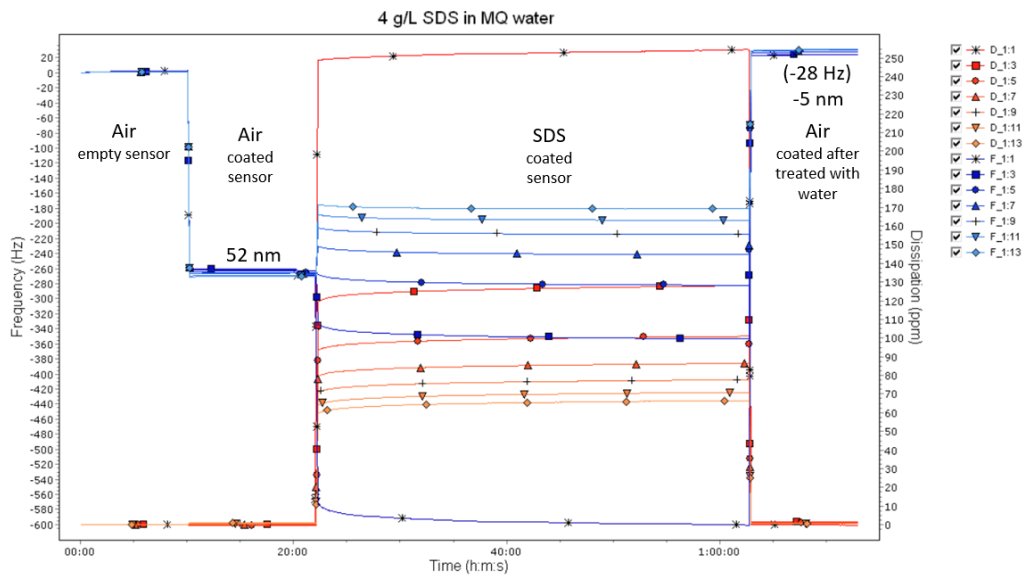


Figure 12: Protocol A for 4 g/L SDS water. Frequency (blue) and dissipation (red) of all overtones is shown. The four regimes are: 1 - empty sensor in air, 2 -sensor with vaseline film (coated) in air, 3 - sensor with vaseline film in SDS solution, 4 – dried sensor after treatment with water. One measurement of each regime is shown. n=1

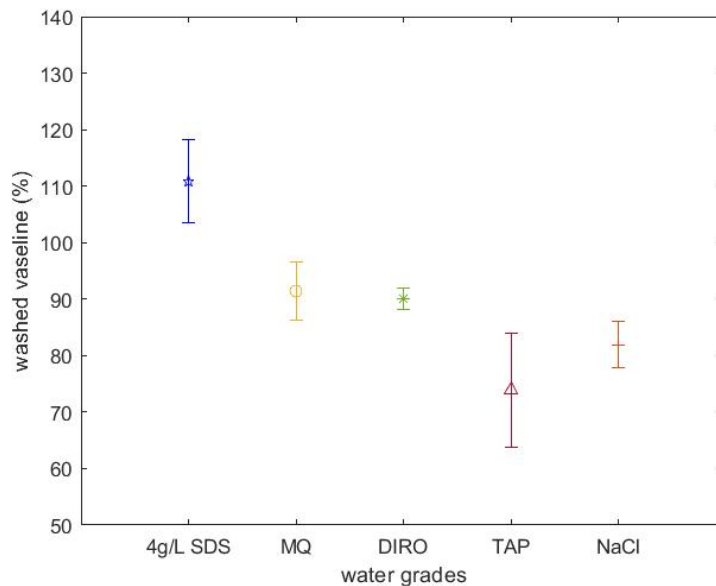


Figure 13: Percent of mean washed vaseline for each water grade.

Measurement of oil film mass before and after water contact

To detect the washing efficiency of the water grades, the *olive oil* film mass before and after water contact was measured in plastic and glass tubes. To simulate a washing procedure, the tubes were vortexed. When glass tubes were used, purified water grades had the best efficiency (> 65%) in comparison to non-purified ones (\approx 50%). In the plastic surface, less than 18% of the olive oil is washed away and there is no substantial difference between the water grades. Moreover, DIRO water shows the most consistent results (figure 14).

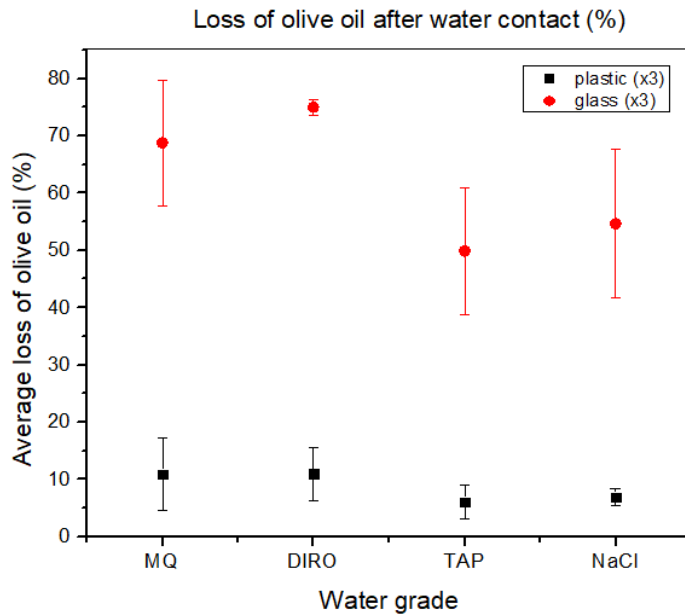


Figure 14: Average loss of olive oil (%) of four different water grades in two materials. Black: plastic, red: glass. The average and standard deviation is shown in the figure. On the x axis are the water grades while on the y axis the average loss of olive oil (%) is found.

Contact angle in a three-phase system (glass surface)

The contact angle of oil droplets in a three-phase system was measured in a glass surface. Results of the contact angle measurements of oil in MQ, DIRO, TAP and 1-20 mM NaCl solutions are shown in figures 15-17. In TAP water (figure 15D) it is observed that the olive oil droplet has the lowest contact angle. Both evaluation methods from figure 16 confirm this finding. The contact angle of olive oil in DIRO and MQ water seems to be similar and higher than the contact angle in TAP water. For the contact angle of hexadecane (figure 17) no significant differences were found. The contact angle was between 70° - 90° for all water grades.

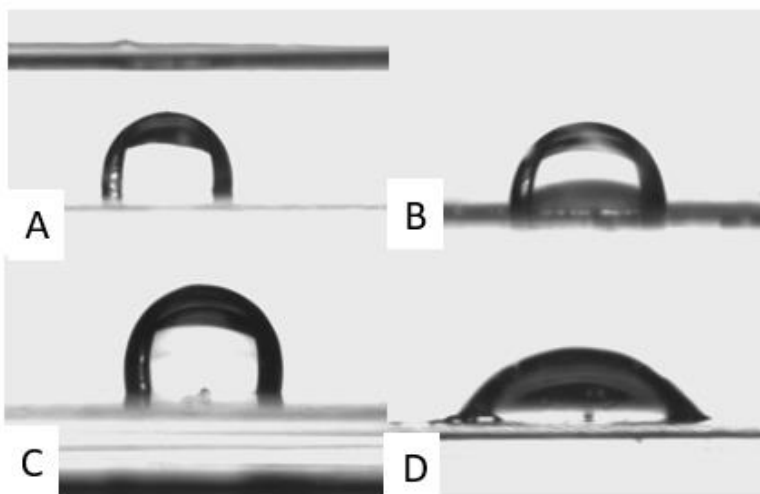


Figure 15: Contact angle of olive oil droplet on glass surface in DIRO (A), MQ (B), NaCl (C) and TAP (D). Photos taken from the Drop Shape Analysis System- DSA100.

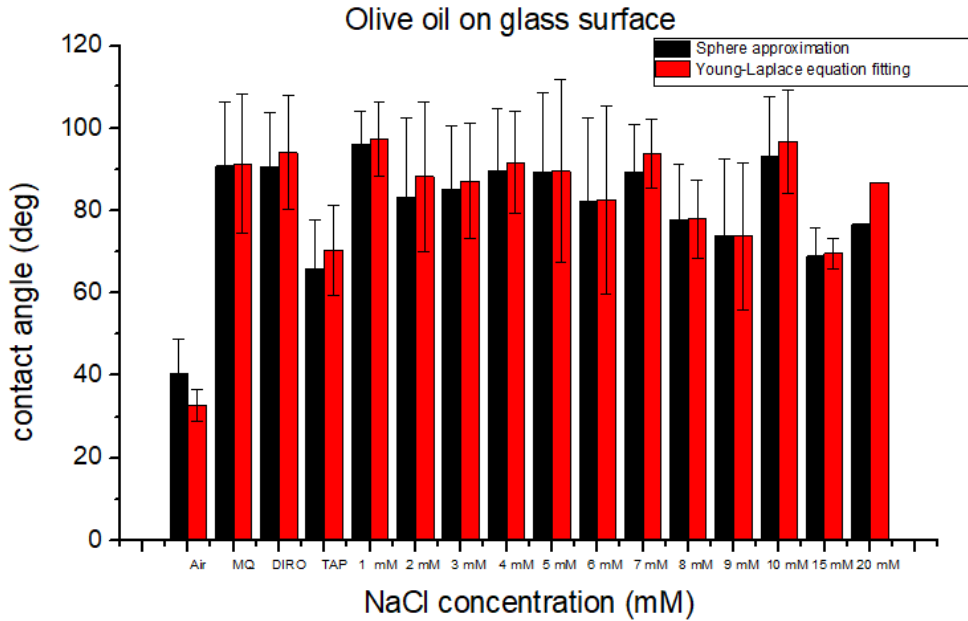


Figure16: Contact angle measurements of 5 μl olive oil droplet in air, MQ, DIRO, TAP and 1-20 mM NaCl in MQ water. Contact angle was measured by two different methods, circle analysis (sphere approximation) in black and drop analysis (Young-Laplace fitting) in red both from ImageJ. $n_{\text{air}} = 16$, $n_{\text{MQ}} = 8$, $n_{\text{DIRO}} = 8$, $n_{\text{TAP}} = 8$, $n_{\text{NaCl}(1-9 \text{ mM})} = 5$, $n_{\text{NaCl}(10 \text{ mM})} = 8$, $n_{\text{NaCl}(15, 20\text{mM})} = 2$

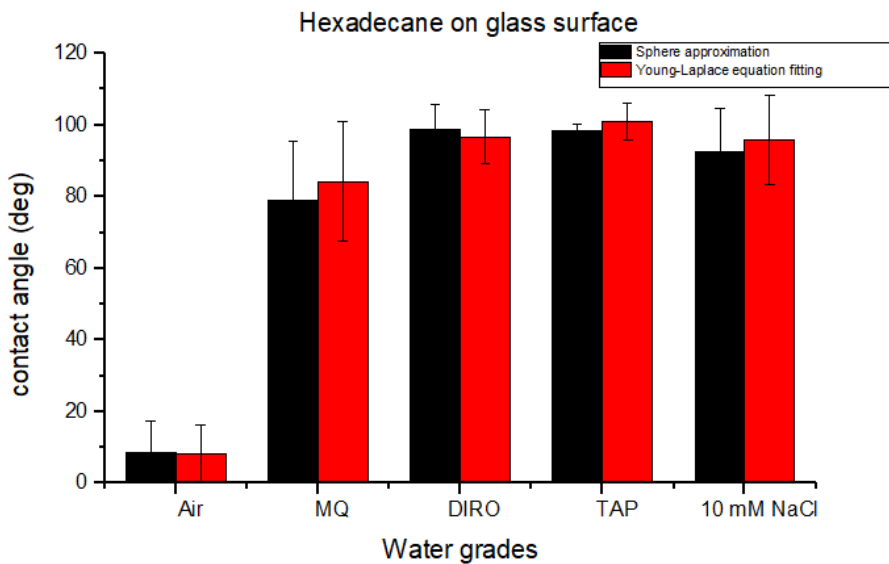


Figure17: Contact angle measurements of 5 μl hexadecane droplet in air, MQ, DIRO, TAP and NaCl. Contact angle was measured by two different analytical methods, circle analysis (sphere approximation) in black and drop analysis (Young-Laplace fitting) in red both from ImageJ. $n=3$.

Spreading of oil on a plastic surface

The contact angle experiment on a plastic surface resulted in a very low, close to zero, angle. Because of that, the area and the thickness of the oil film were measured.

To detect differences between the behavior of the oil phase in the water grades on a plastic surface, the thickness of the oil layer was calculated. The *olive oil layer* is thicker than the *hexadecane layer* (figure 18).

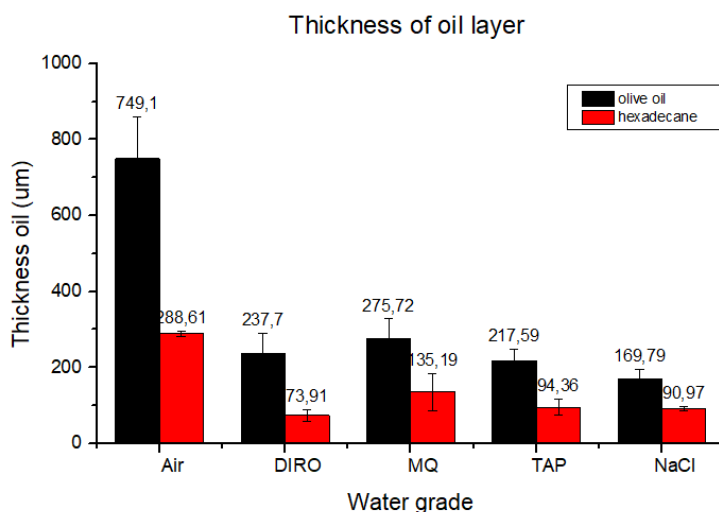


Figure18: Thickness of the oil layer when 5 µl droplets of olive oil (black) and hexadecane (red) are dispersed in air, DIRO, MQ, TAP, NaCl. n=3

Visual observations of the state of oil after emulsification

The state of oil was observed from photos taken from the top and the side of the emulsion. In the first case, the adsorption of the oil was studied while in the latter, the re-emulsification was observed.

Behavior of oil film on a water surface

The state of the oil after the emulsification is seen for four different water grades, two different oils (olive oil and hexadecane) and in two different surfaces, glass and plastic (figures 19-22).

Figures 19 and 20 show the state of the oils in MQ and DIRO water emulsions. In both figures, an accumulation of oil (Oil Red O dispersed in oil) is found in the three-phase line (air, water, surface). In TAP and NaCl samples, the oil accumulation is not visible in all emulsions. Moreover, in the case of TAP and NaCl, the oil forms many small spots in the three-phase system (air, oil, water), which is not visible in the purified water grades (MQ, DIRO). In ‘30 minutes after shaking’ photos, it is observed that the oil in purified water grades does not form a uniform layer while in the non-purified, TAP and NaCl, the oil forms a more continuous layer.

By comparing, hexadecane and olive oil, in all figures is shown that hexadecane emulsions separate faster than the olive oil emulsions.

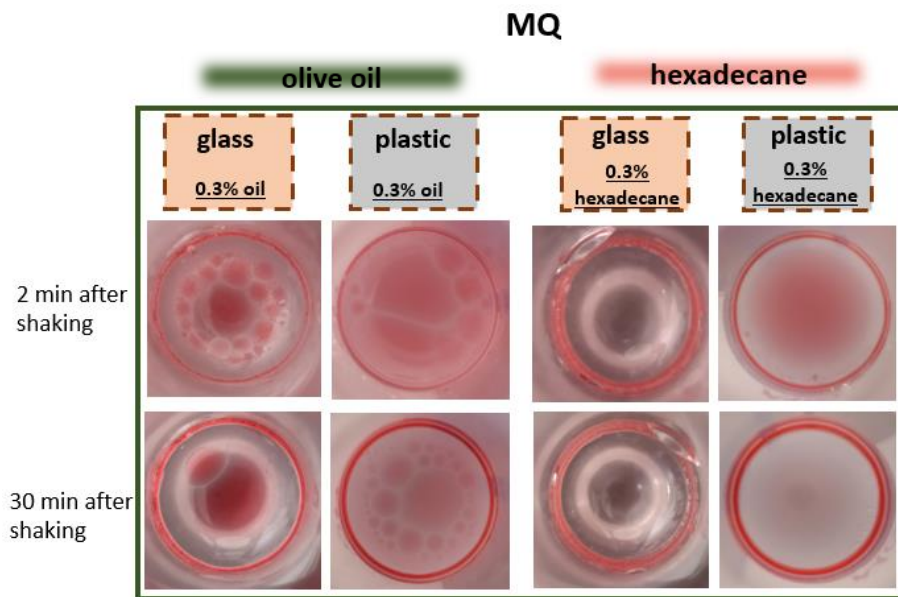


Figure 19: Oil phase after emulsifying 0.3 wt% oil with MQ water in plastic and glass tubes. Photos were taken 2 min and 30 min minutes after emulsification. The red color shows the oil with solubilized red dye. The red circle shows the adsorption of oil in the sides of the tubes. Photos were taken from the top of the emulsion.

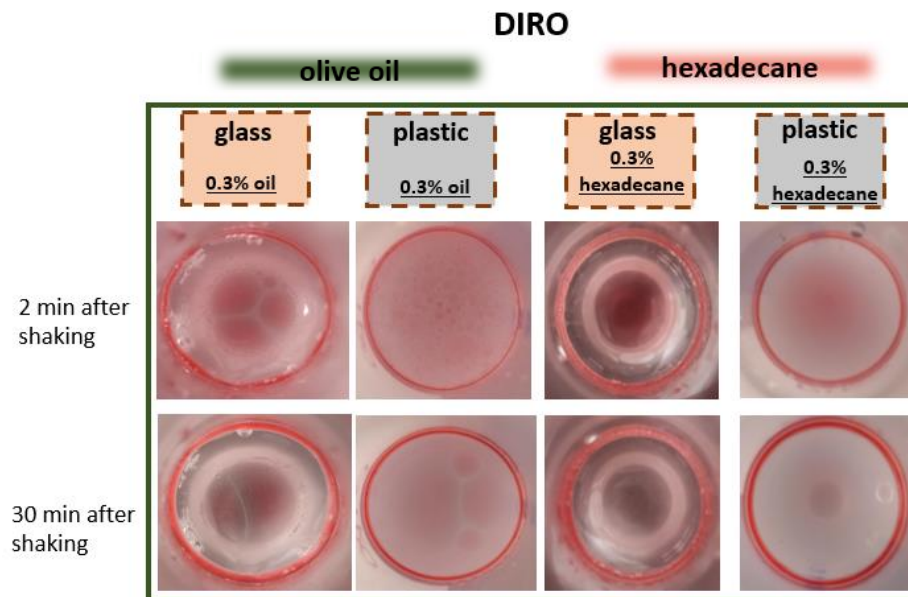


Figure 20: Oil phase after emulsifying 0.3 wt% oil with DIRO water in plastic and glass tubes. Photos were taken 2 min and 30 min minutes after emulsification. The red color shows the oil with solubilized red dye. The red circle shows the adsorption of oil in the sides of the tubes. Photos were taken from the top of the emulsion.

TAP

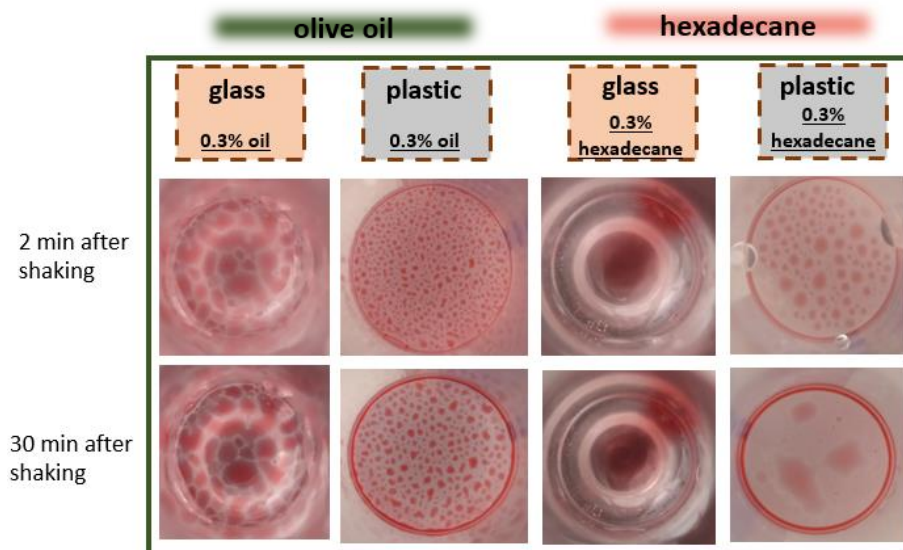


Figure 21: Oil phase after emulsifying 0.3 wt% oil with TAP water in plastic and glass tubes. Photos were taken 2 min and 30 min minutes after emulsification. The red color shows the oil with solubilized red dye. The red circle shows the adsorption of oil in the sides of the tubes. Photos were taken from the top of the emulsion.

NaCl

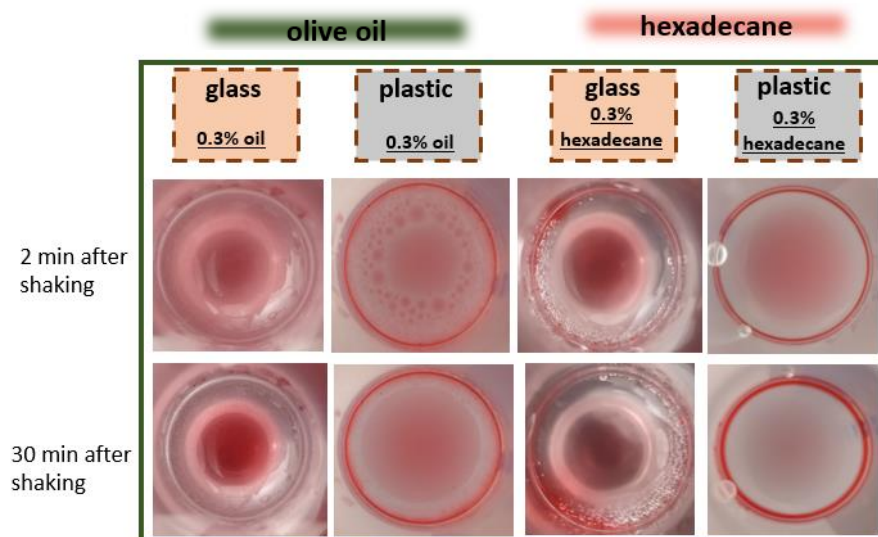


Figure 22: Oil phase after emulsifying 0.3 wt% oil with NaCl in plastic and glass tubes. Photos were taken 2 min and 30 min minutes after emulsification. The red color shows the oil with solubilized red dye. The red circle shows the adsorption of oil in the sides of the tubes. Photos were taken from the top of the emulsion.

Redispersion

After 30 minutes of emulsification, the tubes were gently shaken to observe the redispersion of oil in each water grade. It can be observed that olive oil redisperses more than hexadecane (figures 23,24). By comparing the *olive oil redispersion* in the different water grades (figure 23), it seems that it redisperses in a higher degree in DIRO water. Moreover, when *hexadecane* is used, the redispersion in both MQ and

DIRO results in bigger distinct droplets. TAP and NaCl water seem to not favor redispersion.

Experiments performed in plastic tubes indicate that redispersion is not visible due to adsorption of oil on the plastic walls (data not shown).

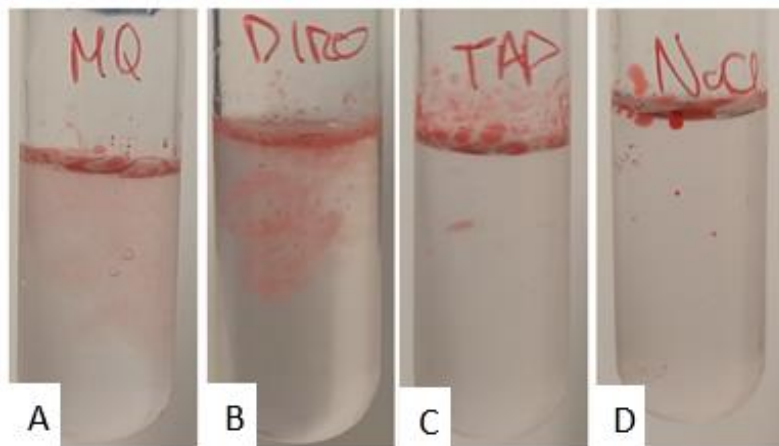


Figure 23: Snapshots from the redispersion videos of olive oil in water in glass tubes. The red color is due to the hydrophobic dye. All emulsions are 0.3 wt% olive oil in MQ (A), DIRO (B), TAP (C) and NaCl (D).

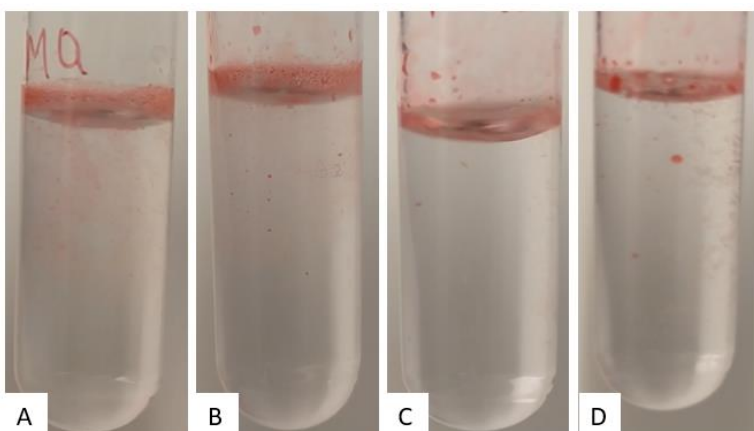


Figure 24: Snapshots from the redispersion videos of hexadecane in water in glass tubes. The red color is due to the hydrophobic dye. All emulsions are 0.3 wt% hexadecane in MQ (A), DIRO (B), TAP (C) and NaCl (D).

Surface and zeta potential of 200 nm and 1 μm particles

To find if pure water has an effect on zeta and surface potential, the zeta potential was measured in a series of NaCl concentrations in MQ water (0-20 mM) for two particle sizes. For 0 mM concentrations, both DIRO and MQ were tested. Results for the 200 nm particles show that with increasing salt concentration, the zeta potential becomes more negative (figure 25, left) while in the 1 μm particles the zeta potential becomes less negative (figure 25, right). By comparing results in the filtrated and non-filtrated solutions it seems that in the 0 mM of the 200 nm particles, there is a difference in the zeta potential. No other substantial difference is found. Moreover, in both figures, there is a steep change of zeta potential in the concentrations between 0-2 mM. In these concentrations, the particle concentration dependency was investigated. Only

non-filtrated NaCl solutions were used for that. The results did not show significant difference (figure 26). The values of each salt concentration were similar to the respective ones from figure 25. In each measurement the size of the particles was also measured (not shown) to ensure that aggregation did not occur.

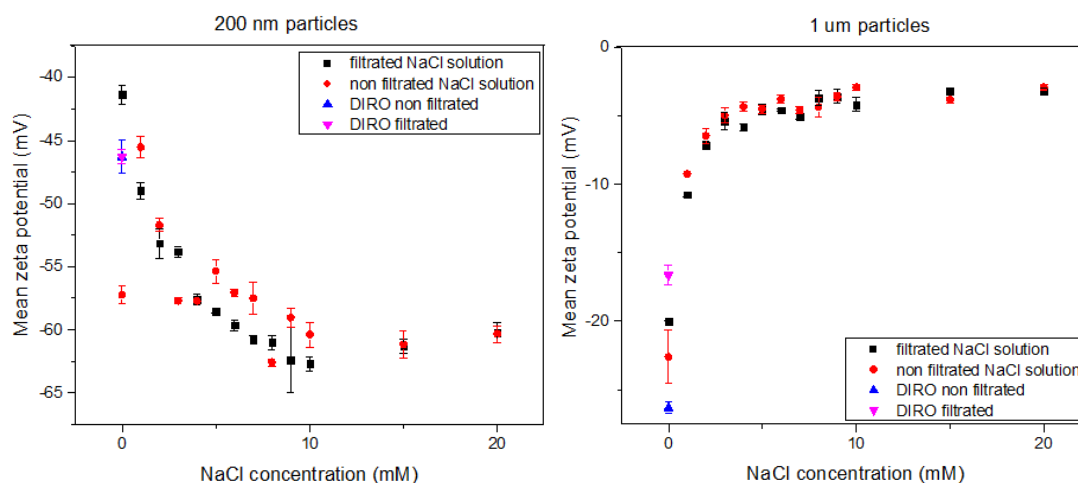


Figure 25: Zeta potential measurement in a series of filtrated and non-filtrated NaCl water (0-20 mM) for 0.1 mg/ml 200 nm particles (left) and 0.05 mg/ml 1 μm particles (right). Emulsions with DIRO water were also measured. n=3

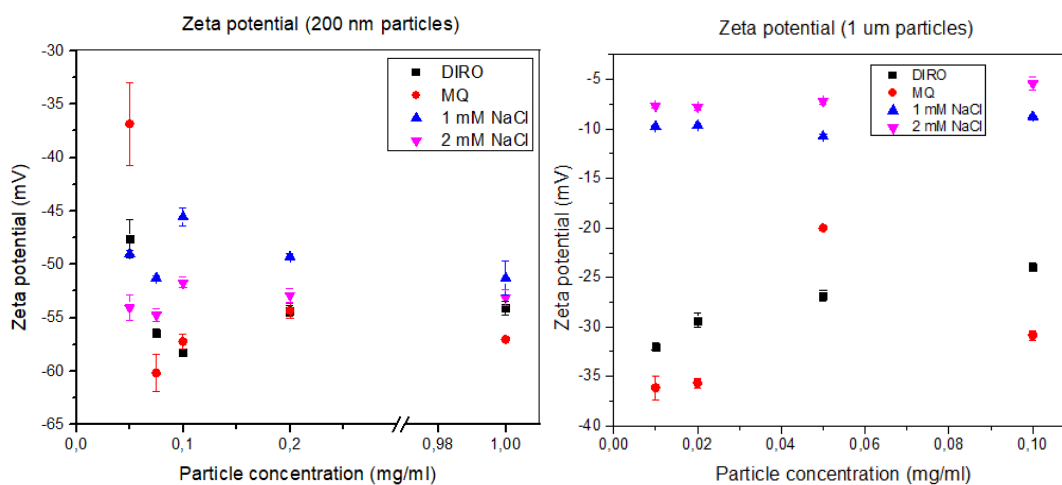


Figure 26: Zeta potential results for non-filtrated NaCl solutions (0-2 mM) in 200 nm particle concentrations: 0.05, 0.075, 0.1, 0.2, 1 mg/ml (left) and in 1 μm particle concentrations 0.01, 0.02, 0.05, 0.1 mg/ml. n=3

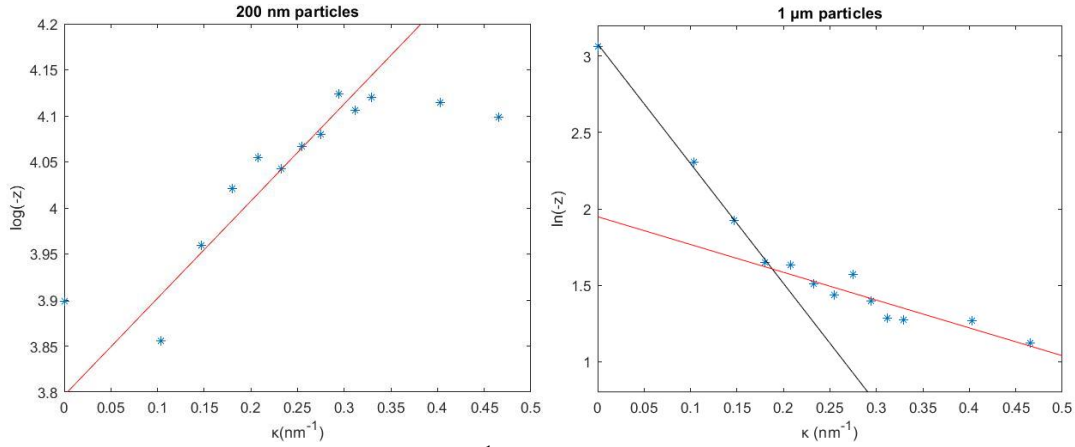


Figure 27: Linear fitting of $\log(-z)$ and κ (nm^{-1}) values of the zeta potential average from filtrated and not filtrated water solutions in 200 nm (left) and 1 μm (right) particles. For 1 μm particles, the data is separated into two linear fitting lines. black line: fitting of 0-3 mM NaCl solution, red line: 4-20 mM NaCl solution. The obtained raw data was analyzed using excel and MATLAB.

Figure 27 shows the linear fitting of the $\log(-z)$ as a function of κ (nm^{-1}) for the 200 nm and 1 μm particles. The figure on the right, shows that for 1 μm particles, 2 regimes are found. The first regime (black line) corresponds to the linear fitting of the first 4 values while the second regime corresponds to the fitting for the rest of the values. For the 200 nm particles (figure 27 left), only one regime is found, and the values do not follow a specific trend.

For 1 μm particles, the surface potential was calculated from the average zeta potential of the filtrated and not filtrated 1 μm particles from protocol 1, as the values did not deviate significantly. In order to calculate it, the Poisson-Boltzmann (PB) equation for spheres was used in the limit of the Debye-Huckel approximation ($|z\psi_0| \leq \kappa T/e \approx 25$ mV) [17,35]. The equation used is:

$$\psi(r, \kappa) = \psi_0 \frac{a}{r} \exp[-\kappa(r - a)] \quad (17)$$

$$\text{where } \kappa^{-1} = \frac{0.3041}{|z|\sqrt{C}} \text{ nm} \quad (18)$$

Where, r is the radial coordinate starting from the center of the particle, a is the particle radius assumed to be 500 nm, ψ_0 is the surface potential, $\psi(r)$ is the potential in distance r and C is concentration for monovalent salts (mol/L). In this case, we assumed that r is the distance to the slipping plane ($r = r_z$) where the zeta potential is found. Another assumption that was made is that the potential does not have a break in the position of the slipping plane.

Eq (17) was re-written as:

$$\ln\psi(r_z, \kappa) = \ln\left(\psi_0 \frac{a}{r_z}\right) + [-\kappa(r_z - a)] \quad (19)$$

Which falls into the $y = \alpha x + \beta$ type. The slope α is equal to $-(r_z - a)$ and β is equal to $\ln(\psi_0 \frac{a}{r_z})$. We assume that r_z is the slipping plane position and that the zeta potential there can be considered as $\psi(r_z, \kappa)$.

For the calculation of surface potential and slipping plane, the slope (α) and the intercept (β) of each regime were used. Figure 27 (right) shows two different regimes. The equation for the low concentration regime (black line) is:

$$y = -7.8354 x + 3.0793 \quad (20)$$

The equation for the high concentration regime (red line) is:

$$y = -1.8183 x + 1.9485 \quad (21)$$

-7.8354 and -1.8183 are both equal to $-(r_z - a)$. From this equality, the slipping plane position (r_z) is equal to 507.83 nm and 501.81 nm for the black and red regime, respectively. $\ln(\psi_0 \frac{a}{r_z})$ is equal to 3.0793 and 1.9485 from equations 20,21. ψ_0 is equal to -22.08 mV and -7.04 mV, respectively. A transition between two linear regimes is found after the 3 mM NaCl sample.

For 200 nm particles the surface potential could not be calculated as the zeta potential values do not obey the DH approximation.

DISCUSSION

A series of experiments was conducted to investigate the fundamentals of using pure water without the addition of surfactant for cleaning and washing procedures. The measurement of oil film mass before and after water contact and the QCM-D experiments were done to detect the washing efficiency of the water grades.

In all cases, a complete or partial removal of oil was detected. Purified water grades showed higher washing efficiency than non-purified TAP water. The efficiency of purified water grades, in the removal of vaseline from a sensor was more than 90% while for TAP it was $\approx 75\%$. In the glass tubes, purified water grades washed away $\approx 70\%$ of the olive oil while TAP, washed away $\approx 50\%$. When the plastic surface was examined, the washing efficiency of purified water grades dropped at 10% and TAP water efficiency at 5%. Results indicate that the washing procedure is more efficient in the silica surface of the sensor and in the glass surface. In the case of NaCl, its efficiency was always higher than TAP water's and lower than the one found in purified water grades. This is because NaCl ions will reduce the Debye screening length by increasing the screening effect; divalent ions, found in TAP water (Ca^{+2} and Mg^{+2}) will have a stronger effect on the reduction of the Debye screening length. This reduction promotes the aggregation of particles. In the case of SDS, 110% of vaseline is washed away. This percentage can be because the sensor thickness tends to decrease after each experiment. At the end of each experiment, after cleaning the

sensor, it is observed that the sensor's frequency is gradually increasing (figure 28). Furthermore, QCM-D results show that the frequency in a water medium does not show substantial changes. Only in the case of SDS, a gradual decrease of the frequency can be observed. In all other water grades the frequencies are linear throughout this regime.

The exact mechanism behind the cleaning process is yet to be investigated since one cannot observe a gradual change of the frequency in the regime where water washes the sensor. It is still unknown whether the surface is cleaned at the time where the medium changes from air to water or it is gradually being cleaned throughout the washing process.

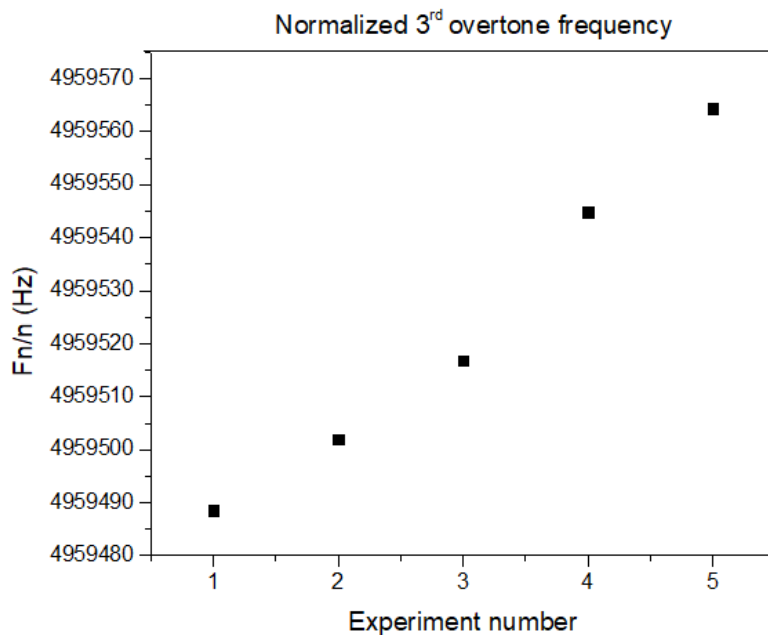


Figure 28: Shift of frequency of the 3rd overtone after each experiment. Mean frequency of five measurements of overtone 3, of an empty sensor in air at the beginning of each experiment.

Olesen et al [36] in their work show the efficiency of various detergents in the washing process. The mechanism that they propose is that the soil is *gradually cleaned* when detergents are used. When the soil first encounters the detergent-water complex it starts to swell, and it is removed gradually. In the swelling step of the process, the frequency decreases fast but when the removal of soil starts to occur, the frequency starts to increase. Results from this master thesis, when SDS detergent was used, show a gradual decrease of the frequency throughout the regime where water washes the sensor. To understand the frequency shifts the properties of the materials used are of great importance. SDS has a density of 1.01 g/cm^3 while vaseline's density is 0.9 g/cm^3 and water has a density of 0.9973 g/cm^3 . When SDS is introduced into the system and starts to remove the vaseline (which has lower density), it forms a bilayer or a multilayer on the surface of the sensor. The thickness of the SDS layers is approximately 5 nm [37]. When a bilayer is formed the thickness would be 10 nm . Then, the addition of this higher density layer on the sensor surface can decrease the frequency.

In the case of washing with purified or non-purified water grades, this decrease is not visible. The sensor at the end is clean but it is unknown how the cleaning process is performed. As mentioned before, when the experiments happen in water medium, the properties of the materials used are of great importance when it comes to frequency shifts. Vaseline has lower density than water and as a material vaseline is also more solid-like. The lower density and the higher firmness that vaseline has can compensate each other and produce the linear trend found in the regime where water washes the sensor. In case of detergent-free cleaning mechanism, further experiments should be done to explain the mechanism behind.

Even though the exact mechanism is not yet clear, it is known that electrostatics are of great importance. It is one of the reasons that builders are used in the detergents. When salt is introduced in an emulsion, the electrostatic interactions between the same charged molecules will decrease and the particles will be prompt to aggregation. In particular, the strength of the electrostatic interactions can be described by the Debye screening length, a parameter that characterizes the distance at which electrostatic interactions still play a role in the interactions between charged particles. When the salt concentration is high, Debye screening length decreases. This decrease will allow the particles to approach or even aggregate. When pure water is used, Debye screening length is higher (1000nm compared to 10 nm in 1mM NaCl solution). This offers stability to the particles and prevents them from aggregation. This mechanism is known as ‘charge stabilization’. Further explanation about the forces that govern this process is found in the DLVO theory that combines electrostatic repulsions with the van der Waals attractive forces and produces a quantitative description of the charge stabilization.

DLVO theory combines the Debye screening length with the surface potential. Since surface potential is hard to find experimentally, the zeta potential was measured for both size particles. Then from zeta potential values, the DLVO theory is always applicable. Because of that, further calculations were done. By using available equations, the surface potential was found from the zeta potential values. Through surface potential, such phenomena as specific adsorption at the particle surface or ionization of the surface groups, can also be studied.

From the surface potential calculation for 1 μm particles, two different regimes were found thus two different equations and surface potential values were shown. Changes between low and high salt content seem to promote the formation of two regimes rather than one. The surface potential value for low salt concentration was -22.08 mV and for high salt concentration it was -7.04 mV. Apart from the different surface potential values, the slipping plane position decreases from 507 nm to 501 nm as the salt concentration increases. The values might be affected by many different factors found in the system such as i) specific adsorption of ions on the particles ii) ionization of surface groups iii) collapse of the polymer conformation on the surfaces due to screening effects iv) more complex equations might need to be used for the system. For example, Giupponi et al [38] mention that the theoretical results of the Debye-Huckel approximation may deviate from the actual results. This may indicate that another equation should be used for high salt concentrations. Ohshima et al [39] have also given an analytical solutions to PB equation by using another approach.

Since the system being examined is quite complex, choosing the correct formulas is a challenge. Overall, the decrease of the slipping plane distance and surface potential might be a result from a combination of the factors mentioned above.

It is known that two main mechanisms are important for the washing and cleaning of liquid soil, and these are: the roll up and the emulsification-solubilization procedures. Contact angle experiments showed that olive oil has a lower contact angle when in TAP water (65° - 70°) while in purified water grades the angle is higher than 90° . It is known that for the roll up mechanism the higher the contact angle the easier it is for the dirt to be washed away [8,40]. As mentioned before, if the contact angle is between 90° and 180° , then mechanical energy needs to be used and the dirt will be washed away. In the case of lower contact angle, mechanical energy alone cannot wash away the dirt completely and a small part of it will remain attached. These findings suggest that in hydrophilic surfaces, such as glass, the purified water grades can form an oil droplet that can easily be washed away with mechanical energy while TAP water alone cannot reach the wanted contact angle. When it comes to the emulsification-solubilization procedure, the redispersion results confirm that the oil phase is more stable in pure water as it redisperses easily. This facilitates the solubilization of soil particles in the emulsion.

Secondary observations such as, surface and particles charge, and the effect of ions were also found to be important for the removal of oil. Both glass and silica surface that are negatively charged in a solution show an easier removal of oil. When, non-purified water grades were used in these surfaces, they induced ions in the emulsion that reduced the electrical potential of the charged surfaces. By reducing the charge, the dirt (oil) can be re-deposited on the surface. These phenomena are limited in the purified water grades. Hydrophobicity was also found to be important for the washing process. Even though purified water grades had again higher efficiency, this number was below 20%, meaning that hydrophobic interactions promote the adsorption of oil on the surface, and it makes it harder to be cleaned.

Differences between the oil phases were also found. Hexadecane spreads more on the plastic surface while olive oil redisperses easier in the water than hexadecane. This drop in the dispersibility may occur due to a change in the conformation of the hexadecane that can reduce its contact with water [41]. Hexadecane is a nonpolar liquid of low surface tension, which is incapable of forming hydrogen bonds. It consists only of CH_2 , CH_3 groups and its cohesive and adhesive properties are simple, since only London dispersion forces are usually involved [42]. This will favor interaction with the polystyrene surface and will increase spreading. On the contrast, olive oil film tends to spread less on the surface. This may be an indication of electrostatic interactions between the fatty acids found in the olive oil. Fatty acids, such as oleic acid, are negatively charged in a water solution. These charges can decrease the interaction of molecules resulting in a more expanded film. Moreover, for the wetting and spreading of a droplet on the surface, electrostatic interactions, van der Waals forces and structural disjoining pressure are important [43]. Depending on the droplet size only one of the forces prevail. Chengara et al. [44] suggest also that it is not only the interfacial tension that is important in the roll-up mechanism but the disjoining pressure also.

Overall, the washing and cleaning process of purified water grades seem to outperform the non-purified water grades in the conditions examined here. In these experiments, there was only one washing cycle. If after one washing cycle, the purified water grades leave 10% of soil on the surface and TAP leaves 25% on, then after 5 washing cycles the pure water grades will leave 90 times less soil on the surface compared to TAP. This means that if a proper washing cycle is designed, a detergent-free washing can become an effective alternative to traditional washing methods.

CONCLUSION

The aim of this study was to examine the removal of oil from surfaces and the effect of water purity on the stability of colloidal systems. QCM-D experiments and measurements of oil film mass before and after water contact were done to examine the removal of soil from surfaces. The stability of colloidal systems was investigated through visual observations of oil in water emulsion, contact angle and spreading measurements. The effect of salt in the zeta potential was investigated by zeta potential measurements. Finally, the following were concluded:

- Both purified and non-purified water grades can remove the oil from a surface but with different efficiency
- Purified water grades wash away the oil phase more efficiently than non-purified water grades
- In purified water grades oil droplets are more stable and can easier be redispersed after creaming
- In purified water grades the contact angle of the olive oil is higher, which can facilitate the roll-up mechanism
- Electrostatic interactions promote removal of oil from negatively charged surfaces

In conclusion, despite the uncertainties of some methods, the combination of these experiments suggests that the washing process can be achieved with the use of only pure water in the systems examined here. The absence of ions in the water, affects the stability of the colloidal systems and facilitates the oil removal from surfaces.

Acknowledgments

First, I would like to express my gratitude to my supervisor Dr. Vitaly Kocherbitov (Professor, Department of Biomedical Science, Faculty of Health and Society, Malmö University) for his support and encouragement throughout my work. Thank you for all the support, interesting meetings, and discussions that we had.

Many thanks to the faculty of Forskaren for helping me with the new techniques and equipment; they were always there to answer my questions.

I would also like to thank, SWATAB for trusting me with this project and made it possible for me to learn more about this topic.

Thank you Manos, for always being there to support me. Konstantina and Chrysoula thank you for always being there for me and supporting me in everything that I do. Thank you Zoi for the funny moments in the lab and for always listening to my non-stop monologues.

Last but not least, I would like to thank my amazing family who is always there for me and supporting me from far. I could not have done all this without their support.

REFERENCES

- [1] P. Ball, *Life's matrix: A biography of water*, 2001.
- [2] K.A. Dill, T.M. Truskett, V. Vlachy, B. Hribar-Lee, Modeling Water, the Hydrophobic Effect, and Ion Solvation, *Annu. Rev. Biophys. Biomol. Struct.* 34 (2005) 173–199. <https://doi.org/10.1146/annurev.biophys.34.040204.144517>.
- [3] S.S. Zumdahl, *Water*, *Encycl. Br.* (1998).
- [4] PubChem, Compound Summary for CID 962, Water., *Natl. Cent. Biotechnol. Inf.* (2021) <https://pubchem.ncbi.nlm.nih.gov/compound/Water>.
- [5] N.R. Pallas, Y. Harrison, An Automated Drop Shape Apparatus and the Surface Tension of Pure Water, *Colloids and Surfaces.* 43 (1990) 169–194.
- [6] Laurén Susanna, Why is surface tension important?, *Biolinscientific.Com.* (2017).
- [7] D. Bajpai, V.K. Tyagi, Laundry detergents: an overview., *J. Oleo Sci.* 56 (2007) 327–340.
- [8] J.A. Poce-Fatou, A superficial overview of detergency, *J. Chem. Educ.* 83 (2006) 1147–1151.
- [9] M.J. Rosen, J.T. Kunjappu, *Phenomena Surfactants and Phenomena*, 2012.
- [10] USGS, Hardness of water, (n.d.) <https://www.usgs.gov/special-topic/water-science-s>.
- [11] A. Porter, *Handbook of Surfactants*, 1991.
- [12] A.L. DeJong, *Textiles*, (1966) 242.
- [13] J.A. Poce-Fatou, M. Bethencourt-Núñez, C. Moreno, J.J. Pinto-Ganfornina, F.J. Moreno-Dorado, A lab experience to illustrate the physicochemical principles of detergency, *J. Chem. Educ.* 85 (2008) 266–268.
- [14] M.F. Cox, Surfactants for hard-surface cleaning: Mechanisms of solid soil removal, *J. Am. Oil Chem. Soc.* 63 (1986) 559–565.
- [15] W. Norde, *Colloids and Interfaces in Life Sciences*, 2003.
- [16] I.W. Hamley, *Introduction to Soft Matter: Polymers, Colloids, Amphiphiles and Liquid Crystals*, 2000.
- [17] J.N. Israelachvili, *Electrostatic Forces between Surfaces in Liquids*, 2011.
- [18] S.T. Hunter, *ZETA POTENTIAL IN COLLOID SCIENCE Principles and Application*, 2014.
- [19] F. Yang, W. Wu, S. Chen, W. Gan, The ionic strength dependent zeta potential at the surface of hexadecane droplets in water and the corresponding interfacial adsorption of surfactants, *Soft Matter.* 13 (2017) 638–646.

<http://dx.doi.org/10.1039/C6SM02174C>.

- [20] G. V. Lowry, R.J. Hill, S. Harper, A.F. Rawle, C.O. Hendren, F. Klaessig, U. Nobbmann, P. Sayre, J. Rumble, Guidance to improve the scientific value of zeta-potential measurements in nanoEHS, *Environ. Sci. Nano.* 3 (2016) 953–965. <http://dx.doi.org/10.1039/C6EN00136J>.
- [21] K. Alias, Emulsion stability, (2013). <https://www.slideshare.net/akarim717/emulsion-stability>.
- [22] B.J. Carroll, Physical aspects of detergency, *Colloids Surfaces A Physicochem. Eng. Asp.* 74 (1993) 131–167.
- [23] C.A. Miller, K.H. Raney, Solubilization-emulsification mechanisms of detergency, *Colloids Surfaces A Physicochem. Eng. Asp.* 74 (1993) 169–215.
- [24] D.J. Shaw, *Colloid and Surface Chemistry*, 4th ed., in: Butterworth–Heinemann Ltd Oxford, 1992: pp. 165, 166.
- [25] Description of the roll-up mechanism can be found at, (n.d.) http://www.scienceinthebox.com/en_UK/glossary/sur.
- [26] E.J.W.& S. E. Matijevic, *Surface and colloid science*, vol. 5, 1972.
- [27] T. Fort, H.R. Billica, T.H. Grindstaff, Studies of soiling and detergency., *J. Am. Oil Chem. Soc.* 45 (1968) 354–361.
- [28] M. Bethencourt, J.A. Poce-fatou, C. Moreno, J.J. Pinto, U. Archaeology, Supplemental Material for Online Publication : A Lab Experience To Illustrate the Physicochemical Principles of Detergency (pp . 1-16) Supplementary material on :, (2008) 1–16.
- [29] D. V. Belsito, A.F. Fransway, J.F. Fowler, E.F. Sherertz, H.I. Maibach, J.G. Mark, C.G.T. Mathias, R.L. Rietschel, F.J. Storrs, J.R. Nethercott, Allergic contact dermatitis to detergents: A multicenter study to assess prevalence, *J. Am. Acad. Dermatol.* 46 (2002) 200–206.
- [30] Bai, H., I. Tam, J. Yu, Contact Allergens in Top-Selling Textile-care Products, 31 (2020) 53–58.
- [31] I. Effendy, H.I. Maibach, Detergent and skin irritation, *Clin. Dermatol.* 14 (1996) 15–21.
- [32] Stadler, Aurélien, D. Sage, Drop Shape Analysis, *Lab. d'imagerie Biomédicale*. (n.d.).
- [33] M. Brugnara, Contact Angle, (2006).
- [34] S. Dill, Ken A.; Bromberg, *Molecular Driving Forces: Statistical Thermodynamics in Chemistry and Biology*, 2003.
- [35] B.C. John, *An introduction to interfaces and colloids. The bridge to nanoscience*, 2010.
- [36] K. Olesen, C. Van Leeuwen, F.I. Andersson, Revealing detergent efficiency and

- mechanism by real-time measurement using a novel and tailored QCM-D methodology, *Tenside, Surfactants, Deterg.* 53 (2016) 488–494.
- [37] Z.Y. Shen, M.T. Lee, On the morphology of the SDS film on the surface of borosilicate glass, *Materials (Basel)*. 10 (2017).
- [38] G. Giupponi, I. Pagonabarraga, Determination of the zeta potential for highly charged colloidal suspensions, *Philos. Trans. R. Soc. A Math. Phys. Eng. Sci.* 369 (2011) 2546–2554.
- [39] H. Ohshima, T.W. Healy, L.R. White, Accurate analytic expressions for the surface charge density/surface potential relationship and double-layer potential distribution for a spherical colloidal particle, *J. Colloid Interface Sci.* 90 (1982) 17–26.
- [40] Miller, C. A., & Raney, K. H. (1993). Solubilization—emulsification mechanisms of detergency. *Colloids and Surfaces A: Physicochemical and Engineering Aspects*, 74(2-3), 169–215. doi:10.1016/0927-7757(93)80263-e, (n.d.).
- [41] C. Tsionopoulos, Thermodynamic analysis of the mutual solubilities of hydrocarbons and water, *Fluid Phase Equilib.* 186 (2001) 185–206.
- [42] E.G. Shafrin, W.A. Zisman, Upper Limits to the Contact Angles of Liquids on Solids, (1964) 145–157.
- [43] D. Wasan, A. Nikolov, K. Kondiparty, The wetting and spreading of nanofluids on solids: Role of the structural disjoining pressure, *Curr. Opin. Colloid Interface Sci.* 16 (2011) 344–349.
- [44] A. Chengara, A.D. Nikolov, D.T. Wasan, A. Trokhymchuk, D. Henderson, Spreading of nanofluids driven by the structural disjoining pressure gradient, *J. Colloid Interface Sci.* 280 (2004) 192–201.